Comparative Analysis Of Transceiver Payload Size Impact On The Performance Of LoRa-Based Sensor Node

Oduoye Israel Olufemi[1]
Department of Electrical and Electronic Engineering
Akwa Ibom State University,
Mkpa Enin Akwa Ibom State Nigeria
oduoyeisrael@gmail.com

Ubong Ukommi[2]
Department of Electrical and Electronic Engineering
Akwa Ibom State University,
Mkpa Enin Akwa Ibom State Nigeria

Emmanuel Ubom[3]
Department of Electrical and Electronic Engineering
Akwa Ibom State University,
Mkpa Enin Akwa Ibom State Nigeria

***Abstract*— In this paper, comparative analysis of transceiver payload size impact on the performance of LoRa-based sensor node is presented. The analytical model for determination of the appropriate payload size for a given sensor node based on the data capture per cycle and duty cycle requirement is presented. Also presented are analytical models for determination of the mean current and energy consumption per cycle, as well as analytical models for battery lifetime, the bit error probability and the transmission range. A case study sensor dataset used for numerical computations consists of the following parameter values: transmitter power of 13 dBm, sensor node cycle time of 1800 seconds, frequency(f) of 868 MHz, bandwidth (BW) of 125 KHz, spreading factor (SF) of 12, payload delivery success ratio (R_{Succ}) $of\ 0.99$, and battery capacity (Bat_{cap}) of 2400 mAh. The payload sizes of 5, 10, 20, 25, 30 and 50 bytes were used and the results show that the packet transmission time increases with payload size with about 52 % change in the packet transmission time within the payload size range considered. Also, the mean current and the total energy consumed decrease with payload size with about -14 % change in the mean current and the total energy within the payload size range considered. Again, the battery life span increases with payload size with about -12 % change in the battery life span within the payload size range considered. The transmission range decreases with payload size with about -5 % change in the transmission range within the payload size range considered. Finally, the bit error probability decreases with payload size with about -900 % change in the bit error probability within the payload size range considered. The results show that the payload size has significant impact on the performance of LoRa transceiver.**

Keywords:* *Transceiver, Bit Error Probability, LoRa, Sensor Node, Payload size

1. INTRODUCTION

Nowadays, with the increasing adoption of LoRa-based wireless sensor networks for Internet of things and smart systems applications researchers are increasing seeking for ways to enhance the performance of the LoRa technology [1,2,3,4]. Notably, LoRa transceiver has several parameters that needs to be properly selected for effective and efficient performance [5,6,7,8,9,10].

Furthermore, sensor nodes are generally resource constrained which requires efficient utilization [11,12,13,14,15]. In some cases, the sensors are battery-powered [16,17,18,19,20]. This requires estimation of the energy consumption of the sensors and the battery lifetime as well as the impact of various parameters on the energy consumption of the sensors and the battery lifetime [21,22,23,24]. Accordingly, in this paper the impact of payload size on the energy consumption of the sensors, the battery lifetime and on other performance parameters of the LoRa-based sensor node are presented [25,26,27,28 The study presented analytical approach for selecting appropriate payload size for LoRa-based sensor node and then evaluate the impact of varying the payload size on the performance of the sensor node.

2. METHODOLOGY

When the sensor units in a LoRa-based sensor node capture data in each cycle the LoRa transceiver need to transmit all the data within the sensor node cycle time. Consider a case where the sensor units in a node that generate a total useful payload data, denoted as TTLPayLd per cycle with sensor node cycle time, denoted as $t_{SNCycle}$, the LoRa transceiver can deliver the TTLPayLd with transmitter payload size, denoted as PayLdUsFl, such that the whole TTLPayLd sensor data per cycle is transmitted in n_{LRtx} number of transmissions per cycle, where;

$$n_{LRtx} = \left\lceil \frac{TTLPayLd}{PayLdUsFl} \right\rceil \quad (1)$$

where ⌈.⌉ means round up to the nearest integer; for instance, ⌈2.4⌉ gives 3. The LoRa transceiver transmission repeat time or the transmitter cycle time, denoted as $t_{LRtxCycle}$ is therefore given as;

$$t_{LRtxCycle} = \frac{t_{SNCycle}}{n_{LRtx}} \quad (2)$$

Usually, LoRa transceivers have duty cycle restriction which in most cases requires that the LoRa transceiver duty cycle should not exceed 1%. In that case, the LoRa transmission time (denoted as t_{LRtx}) for the useful payload size of PayLdUsFl should not exceed 1 % of $t_{LRtxCycle}$. Hence,

$$t_{LRtx} \leq 0.01(t_{LRtxCycle}) \quad (3)$$

For a LoRa with useful payload size of PayLdUsFl, the packet transmission time, t_{LRtx} for a spreading factor (denoted as SF) is computer as follows;

$$t_{LRtx} = (n_{PL} + n_{PR} + 4.25)\left(\frac{2^{SF}}{BW}\right) \quad (4)$$

where n_{PR} is the size of the preamble in the packet. For the case study n_{PR} =8 [29];

BW is the bandwidth, (BW can have values of 125 KHz, 250 KHz or 500 KHz). For the case study BW =125 KHz;

H is the header flag (H can have value of 0 when enabled or 1 when disabled). For the case study H =0;

DE is the low data rate optimization flag (D can have value of 1 when enabled or 0 when disabled). For the case study DE =1;

CR is the coding rate (CR can have values of 1, 2, 3, or 4). For the case study CR =1;

CRC = 1 for uplink and= 0 for down link. For the case study CRC =1;

PL is the total payload size including the useful payload (denoted as PayLdUsFl) and all the header bytes (denoted as *Header*) which are overheads, hence;

$$PL = \text{PayLdUsFl} + Header \quad (5)$$

$$n_{PL} = 8 + max\left(\left(ceil\left[\frac{8(PL) - 4(SF) + 28 + 16\,(CRC) - 20(H)}{4(SF - 2(DE))}\right](CR + 4)\right), 0\right) \quad (6)$$

Then, for a case study sensor node with 4 states, as shown in Table 1, the sleep state time denoted as Tsleep is given as;

$$\text{Tsleep} = t_{SNCycle} - \sum_{x=1}^{x=4}(t_x) \quad (7)$$

The mean current, I_{MN} drawn by the sensor node per cycle and the energy consumed per cycle, E_{cycl} are given as;

$$I_{MN} = \frac{\sum_{x=1}^{x=4}((I_x)(t_x))}{\sum_{x=1}^{x=4}(t_x)} \quad (8)$$

$$E_{cycl} = I_{MN}(V_{SN})(t_{SNCycle}) \quad (9)$$

where V_{SN} is the voltage of the sensor node.

Table 1 The sensor node state current and time parameters for the case study sensor node

Sensor node state number , x	Description of sensor node state	Symbol for the duration	Duration (ms)	Symbol for the current	Current (mA)
1	Transmission	t_1	t_{LRtx} given in Equation 4	I_1	83.113
2	Receive data	t_2	504.081	I_2	31.913
3	Measure state and other states	t_3	31050.67	I_3	45.500
4	Sleep	t_4	Tsleep given in Equation 7	I_4	0.158

With battery capacity, Bat_{cap} in mAh, the sensor node battery lifespan Bat_{lfTm} in hours can be estimated as;

$$Bat_{lfTm} = \frac{Bat_{cap}}{I_{MN}} \quad (10)$$

where I_{MN}isin mA. If the targeted payload delivery success ration, R_{Succ} is given, then the actually delivered useful payload size, denoted as PayLdUsFlDLVD is given as as,

$$\text{PayLdUsFlDLVD} = R_{Succ}(\text{PayLdUsFl}) \quad (11)$$

Then, the bit error probability, BEP is obtained as follows;

$$\text{BEP} = 1 - \left(\left[\frac{R_{Succ}}{(1 - PMAC_{coll})}\right]^{\left(\left(\frac{5}{4}\right)(\text{TTLPayLd} - \text{Header})\right)^{-1}}\right) \quad (12)$$

where $PMAC_{coll}$ is the probability that a packet collision occurred in the media access control layer. In this work, $PMAC_{coll}$ is set to 0 and *Header* is set to 13 bytes, hence,

$$\text{BEP} = 1 - \left([R_{Succ}]^{\left(\left(\frac{5}{4}\right)(\text{TTLPayLd} - 13)\right)^{-1}}\right) \quad (13)$$

The energy per bit to noise power spectral density is denoted as E_b/N_O, and for LoRa modulation scheme with spreading factor, SF, the value of E_b/N_O is obtained as;

$$E_b/N_O = \frac{erfinv(1 - 2(BEP))}{\left(\frac{\log_{12}(SF)}{\sqrt{2}}\right)} \quad (12)$$

The value of E_b/N_O in dBm is given as;

$$\left.\frac{E_b}{N_0}\right|_{dB} = 10\,Log\left(E_b/N_O\right) \quad (14)$$

The link margin, LM for LoRa is given as;

$$\text{LM} = \left.\frac{E_b}{N_0}\right|_{dB} + 10\log_{10}(SF) + 10\log_{10}\left(\frac{4}{4 + CR}\right) - 10\log_{10}(2^{SF}) - LR_{sens} - 174 + 10\log_{10}(BW) + NF \quad (15)$$

where LR_{sens} is the LoRa receiver sensitivity and NF is the noise figure. For a modified free space path loss with path loss exponent of 3 rather than 2, the transmission range, d is given as,

$$d = 10^{\left(\frac{P_t - LR_{sens} - LM - 32.5 - 30\log_{10}(f)}{30}\right)} \quad (16)$$

where P_t is the transmitter power in dBm and f is is the signal frequency in MHz.

3. RESULTS AND DISCUSSION

A case study sensor dataset used for numerical computations consists of the following parameter values: P_t = 13 dBm, sensor node cycle time of 1800 seconds, f =868 MHz, BW =125 KHz, NF = 6 dBm, CR =1, SF =12, $LR_{sens} = -137\ dBm$, $PMAC_{coll} = 0$, $R_{Succ} = 0.99$, V_{SN} =3.6 V and Bat_{cap} = 2400 mAh. The payload sizes of 5, 10, 20, 25, 30 and 50 bytes are used and the results obtained for the packet transmission time versus payload are shown in Figure 1. The results in Figure 1 show that the packet transmission time increases with payload size with about 52 % change in the packet transmission time within the payload size range considered. The results in Figure 2 show that the mean current decreases with payload size with about -14 % change in the mean current within the payload size range considered. The results in Figure 3 show that the total energy consumed per cycle decreases with payload size with about -14 % change in the total energy consumed within the payload size range considered. The results in Figure 4 show that the battery life span increases with payload size with about -12 % change in the battery life span within the payload size range considered. The results in Figure 5 show that the energy per useful bit decreases with payload size with about -1044 % change in the energy per useful bit within the payload size range considered. The results in Figure 6 show that the transmission range decreases with payload size with about -5 % change in the transmission range within the payload size range considered. The results in Figure 7 and Figure 8 show that the bit error probability decreases with payload size with about -900 % change in the bit error probability within the payload size range considered.

In all, the results show that increasing payload size improves the energy efficiency of the node but reduces the transmission range. As such, the choice of payload size is a compromise between energy efficient system and longer transmission range. In addition, the results in Figure 9 show that only payload size of 50 bytes and above satisfied the 1 % duty cycle requirement. So, for the case study sensor node, payload size lower than 50 bytes will not be used where the 1% duty cycle restriction applies.

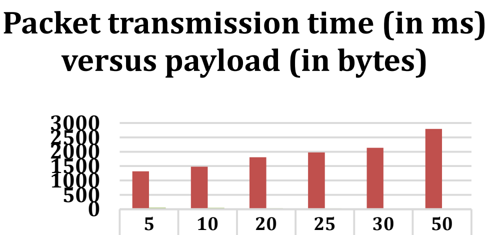

	5 Bytes	10 Bytes	20 Bytes	25 Bytes	30 Bytes	50 Bytes
Packet transmission time (in ms) versus payload (in bytes)	1319	1483	1810	1974	2138	2793
Percentage change with respect to that of the 50 byte payload (%)	52.79	46.92	35.19	29.33	23.46	0.00

Figure 1 The bar chart for the packet transmission time versus payload

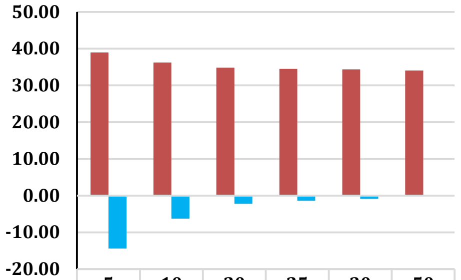

	5 Bytes	10 Bytes	20 Bytes	25 Bytes	30 Bytes	50 Bytes
Mean current (in mA) versus payload (in bytes)	38.98	36.21	34.82	34.54	34.36	34.06
Percentage change with respect to that of the 50 byte payload (%)	-14.43	-6.29	-2.22	-1.41	-0.87	0.00

Figure 2 The bar chart for the mean current versus payload

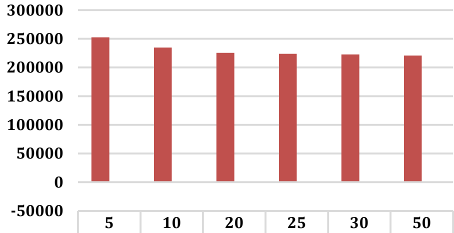

	5 Bytes	10 Bytes	20 Bytes	25 Bytes	30 Bytes	50 Bytes
Total Energy Consumed per Cycle (in µJ) versus payload (in bytes)	252588	234627	225646	223850	222653	220741
Percentage change with respect to that of the 50 byte payload (%)	-14.43	-6.29	-2.22	-1.41	-0.87	0.00

Figure 3 The bar chart for the total energy consumed per cycle versus payload

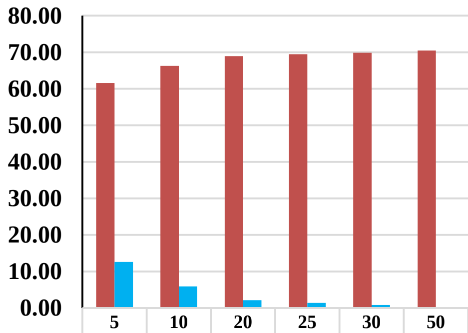

	5 Bytes	10 Bytes	20 Bytes	25 Bytes	30 Bytes	50 Bytes
Battery Life (in hr) versus payload (in bytes)	61.57	66.28	68.92	69.47	69.85	70.45
Percentage change with respect to that of the 50 byte payload (%)	12.61	5.92	2.17	1.39	0.86	0.00

Figure 4 The bar chart for the battery life span versus payload

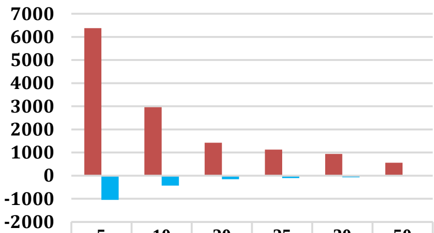

	5 Bytes	10 Bytes	20 Bytes	25 Bytes	30 Bytes	50 Bytes
Energy per useful bit (in µJ/bit) versus payload (in bytes)	6378	2962	1425	1131	937	557
Percentage change with respect to that of the 50 byte payload (%)	-1044	-431	-156	-103	-68	0

Figure 5 The bar chart for the transmission range versus payload

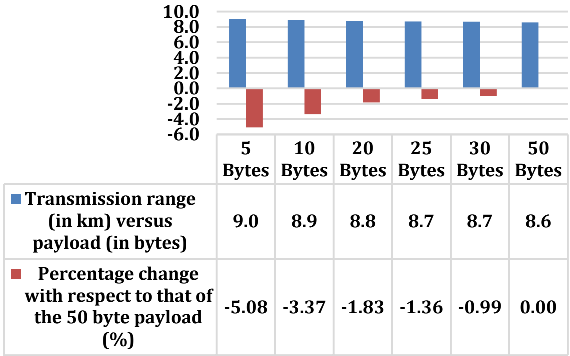

Figure 6 The bar chart for the transmission range versus payload

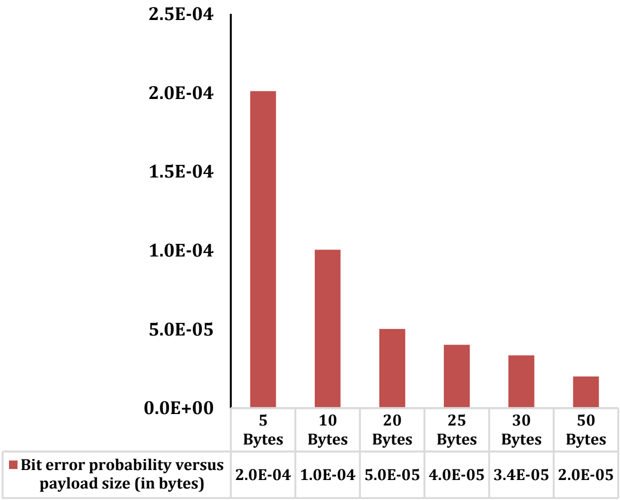

Figure 7 The bar chart for the bit error rate versus payload

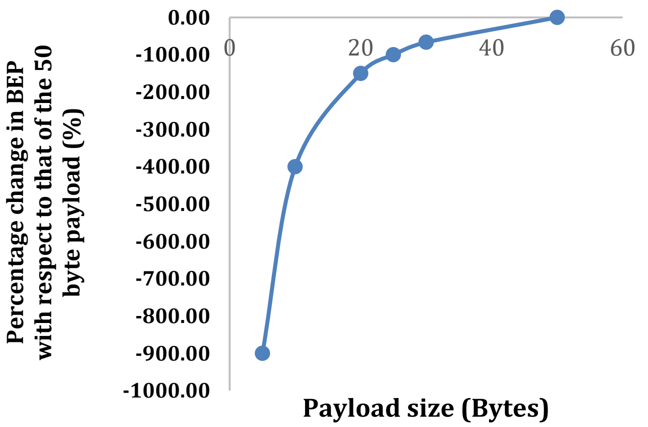

Figure 8 The graph of percentage change in BEP with respect to that of the 50 byte payload (%)

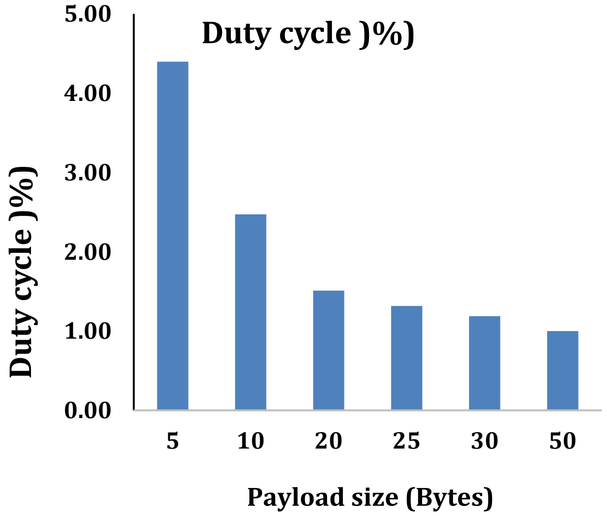

Figure 9 The graph of duty cycle versus payload size

4 CONCLUSION

The effect of transmitter payload size on the energy consumption and related performance parameters for a sensor node employing LoRa transceiver is presented. The mathematical expressions for the computation of the various LoRa sensor node performance parameters as function of the payload size are presented. The study considered LoRa transceiver operating with spreading factor of 12 and payload size ranging from 5 bytes to 50 bytes. The results of sample numerical computations show that the higher payload size improves energy efficiency and while the smaller payload size is suitable for long transmission range. In all, the choice of payload size is based on the compromise between transmission range and energy efficiency.

REFERENCES

1. Saban, M., Bekkour, M., Amdaouch, I., El Gueri, J., Ait Ahmed, B., Chaari, M. Z., ... & Aghzout, O. (2023). A Smart Agricultural System Based on PLC and a Cloud Computing Web Application Using LoRa and LoRaWan. *Sensors*, *23*(5), 2725.
2. Pagano, A., Croce, D., Tinnirello, I., & Vitale, G. (2022). A Survey on LoRa for Smart Agriculture: Current Trends and Future Perspectives. *IEEE Internet of Things Journal*, *10*(4), 3664-3679.
3. Mao, W., Zhao, Z., Chang, Z., Min, G., & Gao, W. (2021). Energy-efficient industrial internet of things: Overview and open issues. *IEEE transactions on industrial informatics*, *17*(11), 7225-7237.
4. Abdollahi, A., Rejeb, K., Rejeb, A., Mostafa, M. M., & Zailani, S. (2021). Wireless sensor networks in agriculture: Insights from bibliometric analysis. *Sustainability*, *13*(21), 12011.
5. Alves, A. E. S., Pires, L. M. R., & Gonçalves, L. C. (2023). CSMA Protocol performance with dynamic spreading factor in LPWAN networks with LoRa RF transceivers. *Brazilian Journal of Development*, *9*(05), 18569-18579.
6. Askhedkar, A. R., & Chaudhari, B. S. (2023). Multi-Armed Bandit Algorithm Policy for LoRa Network Performance Enhancement. *Journal of Sensor and Actuator Networks*, *12*(3), 38.

7. Malik, P., Bilandi, N., & Gupta, A. (2022). Narrow band-IoT and long-range technology of IoT smart communication: Designs and challenges. *Computers & Industrial Engineering*, 108572.
8. Gkotsiopoulos, P., Zorbas, D., & Douligeris, C. (2021). Performance determinants in LoRa networks: A literature review. *IEEE Communications Surveys & Tutorials*, *23*(3), 1721-1758.
9. Sciullo, L., Trotta, A., & Di Felice, M. (2020). Design and performance evaluation of a LoRa-based mobile emergency management system (LOCATE). *Ad Hoc Networks*, *96*, 101993.
10. Azhar Muzafar, M. I. Z., Mohd Ali, A., & Zulkifli, S. (2022). A study on lora sx1276 performance in iot health monitoring. *Wireless Communications and Mobile Computing*, *2022*.
11. Bhushan, B., & Sahoo, G. (2020). Requirements, protocols, and security challenges in wireless sensor networks: An industrial perspective. *Handbook of computer networks and cyber security: principles and paradigms*, 683-713.
12. Gulati, K., Boddu, R. S. K., Kapila, D., Bangare, S. L., Chandnani, N., & Saravanan, G. (2022). A review paper on wireless sensor network techniques in Internet of Things (IoT). *Materials Today: Proceedings*, *51*, 161-165.
13. Chaudhari, B. S., Zennaro, M., & Borkar, S. (2020). LPWAN technologies: Emerging application characteristics, requirements, and design considerations. *Future Internet*, *12*(3), 46.
14. Pincheira, M., Vecchio, M., Giaffreda, R., & Kanhere, S. S. (2020, May). Exploiting constrained IoT devices in a trustless blockchain-based water management system. In *2020 IEEE International Conference on Blockchain and Cryptocurrency (ICBC)* (pp. 1-7). IEEE.
15. Wang, D., Wang, P., & Wang, C. (2020). Efficient multi-factor user authentication protocol with forward secrecy for real-time data access in WSNs. *ACM Transactions on Cyber-Physical Systems*, *4*(3), 1-26.
16. Subbaramaiah, R., Al-Jufout, S. A., Ahmed, A., & Mozumdar, M. M. (2020). Design of vibration-sourced piezoelectric harvester for battery-powered smart road sensor systems. *IEEE Sensors Journal*, *20*(23), 13940-13949.
17. Hribar, J., DaSilva, L. A., Zhou, S., Jiang, Z., & Dusparic, I. (2022). Timely and sustainable: Utilising correlation in status updates of battery-powered and energy-harvesting sensors using deep reinforcement learning. *Computer Communications*, *192*, 223-233.
18. Noh, Y. S., Seo, J. I., Choi, W. J., Kim, J. H., Van Phuoc, H., Kim, H. S., & Lee, S. G. (2021, February). 17.6 A Reconfigurable DC-DC Converter for Maximum TEG Energy Harvesting in a Battery-Powered Wireless Sensor Node. In *2021 IEEE International Solid-State Circuits Conference (ISSCC)* (Vol. 64, pp. 266-268). IEEE.
19. Portilla, L., Loganathan, K., Faber, H., Eid, A., Hester, J. G., Tentzeris, M. M., ... & Pecunia, V. (2023). Wirelessly powered large-area electronics for the Internet of Things. *Nature Electronics*, *6*(1), 10-17.
20. Gupta, S., Gupta, S., & Goyal, D. (2021). Comparison of Q-coverage P-connectivity sensor node scheduling heuristic between battery powered WSN & energy harvesting WSN. *International Journal of Sensors Wireless Communications and Control*, *11*(5), 553-559.
21. Spathi, K. P., Beletsioti, G. A., Kantelis, K. F., Valkanis, A., Nicopolitidis, P., & Papadimitriou, G. I. (2023). Increasing device energy efficiency in LoRaWAN networks via a learning-automata-based approach. *International Journal of Sensor Networks*, *42*(2), 87-101.
22. Sarhaddi, F., Azimi, I., Labbaf, S., Niela-Vilén, H., Dutt, N., Axelin, A., ... & Rahmani, A. M. (2021). Long-term IoT-based maternal monitoring: system design and evaluation. *Sensors*, *21*(7), 2281.
23. Kuaban, G. S., Gelenbe, E., Czachórski, T., Czekalski, P., & Tangka, J. K. (2023). Modelling of the Energy Depletion Process and Battery Depletion Attacks for Battery-Powered Internet of Things (IoT) Devices. *Sensors*, *23*(13), 6183.
24. Amutha, J., Sharma, S., & Nagar, J. (2020). WSN strategies based on sensors, deployment, sensing models, coverage and energy efficiency: Review, approaches and open issues. *Wireless Personal Communications*, *111*, 1089-1115.
25. Väänänen, O., & Hämäläinen, T. (2021, June). LoRa-based sensor node energy consumption with data compression. In *2021 IEEE International Workshop on Metrology for Industry 4.0 & IoT (MetroInd4. 0&IoT)* (pp. 6-11). IEEE.
26. Väänänen, O., & Hämäläinen, T. (2021, June). LoRa-based sensor node energy consumption with data compression. In *2021 IEEE International Workshop on Metrology for Industry 4.0 & IoT (MetroInd4. 0&IoT)* (pp. 6-11). IEEE.
27. Väänänen, O., & Hämäläinen, T. (2022). Efficiency of temporal sensor data compression methods to reduce LoRa-based sensor node energy consumption. *Sensor Review*, *42*(5), 503-516.
28. Adi, P. D. P., & Kitagawa, A. (2020, August). Performance evaluation of low power wide area (LPWA) LoRa 920 MHz sensor node to medical monitoring IoT based. In *2020 10th Electrical Power, Electronics, Communications, Controls and Informatics Seminar (EECCIS)* (pp. 278-283). IEEE.
29. Rúni Eriksen () Energy Consumption of Low Power Wide Area Network Node Devices in the Industrial, Scientific and Medical Band